Representation of Imprecise Digital Shapes

Isabelle Sivignon *

Univ. Grenoble Alpes, GIPSA-Lab, F-38000 Grenoble, France
CNRS, GIPSA-Lab, F-38000 Grenoble, France
isabelle.sivignon@gipsa-lab.grenoble-inp.fr

Abstract. In this paper, we investigate a new framework to handle noisy digital shapes. Given a ground truth continuous shape which contour is a simple closed curve, we consider the digital shape obtained after any digital conversion (scan, picture, etc). A digital imprecise contour is a simple 4-connected closed digital curve, such that an imprecision value is known for each point. This imprecision value stands for the radius of a ball around the point, such that the ground truth contour lies in the union of all the balls. In the first part, we show how to define an imprecise digital shape from such an imprecise digital contour. To do so, we define three classes of points : inside points, outside points and uncertain points. In the second part of the paper, we build on this definition for a volumetric analysis of imprecise digital shapes. From so-called toleranced balls, a filtration of shapes, called λ-shapes is defined. We show how to define a set of sites to encode this filtration of shapes.

Keywords: Digital geometry, imprecision, contour, shape analysis

1 Introduction

Whatever the quality of the sensor of the acquisition device, digital images are always intrisically "noisy" because of the discretization of the real data on a regular grid. When image analysis focuses on the shapes contained in it, the segmentation step used to extract the shapes further increases this phenomenon. Many approaches have been proposed over the years in order to deal with the noise during digital shapes analysis. Some approaches introduce a global "thickness" parameter that is used to twarth the noise effect [6]. This has two important drawbacks: first, digital shapes with non uniform amount of noise are not handled correctly because of the global parameter - important details in smooth parts of the object may be lost; second, cancelling the noise effect is somehow a loss of information as an ill-defined denoised shape is implicitely studied. Instead of analysing one possible denoised shape by mean of the global parameter, why not analysing all the possible shapes at once ?

In the last decade, many researches have been conducted on imprecise or uncertain data and related geometric problems. The terms "imprecise" [12] and

* This work was partially founded by the French *Agence Nationale de la Recherche* (Grant agreement ANR-11-BS02-009)

"uncertain" [8] or "fuzzy" [11, 14] data can be found in the literature : uncertain or fuzzy data is endowed with a probabilistic information, while imprecise data only contains geometric information. In this work, we will focus on imprecise data : each point is then replaced by a *region* that models the imprecision.

Dealing with imprecise data has been an active field in computational geometry recently [12]. Results concern for instance upper and lower bounds on geometric quantities (smallest enclosing balls, area of convex hull), or pre-processing of geometric structures (Delaunay triangulation). In digital geometry, geometric predicates on digital segments (concurrency, parallelism) were introduced in the context of imprecise data in [15].

In this paper, we present a general framework that lays the foundations for a geometrical analysis of imprecise digital contours and imprecise digital shapes that integrates the imprecision instead of discarding it. In Section 2, we show how to compute an imprecise digital shape from an imprecise closed digital contour. Then, in a second part, we show how to define a family of shapes from an imprecise digital shape, and how to encode this family.

2 From an Imprecise Digital Contour to an Imprecise Digital Shape

Let $\mathcal{C}$ be a simple closed 4-connected digital curve, which is the boundary of a digital shape $\mathcal{S}$. In our framework we assume that the process that led to $\mathcal{C}$ (image acquisition, image segmentation) is not perfect, so that the actual ground truth original contour $\mathcal{C}_0$ is not exactly $\mathcal{C}$ but somewhere close to $\mathcal{C}$.

In order to model the result of this imprecise process, we define the input data as follows. We suppose that with each point p_i of the digital curve $\mathcal{C}$, a positive integer weight r_i is given, so that the input data is an ordered set of weighted points (p_i, r_i), $i \in [0, n[$, $p_i \in \mathbb{Z}^2$, $r_i \in \mathbb{Z}^+$. This weight stands for the confidence in the input data at this point: the greater the weight, the more imprecise the contour around this point. Points p_i for which the position is exact (point p_i belongs to $\mathcal{C}_0$) are assigned with a weight equal to one. More precisely, the weight of the point p is the radius of an open Euclidean ball centered on p, such that the curve $\mathcal{C}_0$ may actually go through the digital points in this ball. The digital curve $\mathcal{C}$ together with the weights is called an *imprecise digital contour*. An illustration of an imprecise digital contour is depicted in Figure 1. In this part, we see how to define an imprecise digital shape from this imprecise contour. *A posteriori* computation of noise level (called meaningful scale) for each point of a digital contour has been proposed in [9]. The data computed using the proposed approached [10] will be used to test our algorithms. The goal here is to identify each point as *inside*, *outside*, or *uncertain*, depending on whether the shape enclosed by $\mathcal{C}_0$ may include the point or not. A precise definition and characterization of these points needs some more work, which is developed in the following pages.

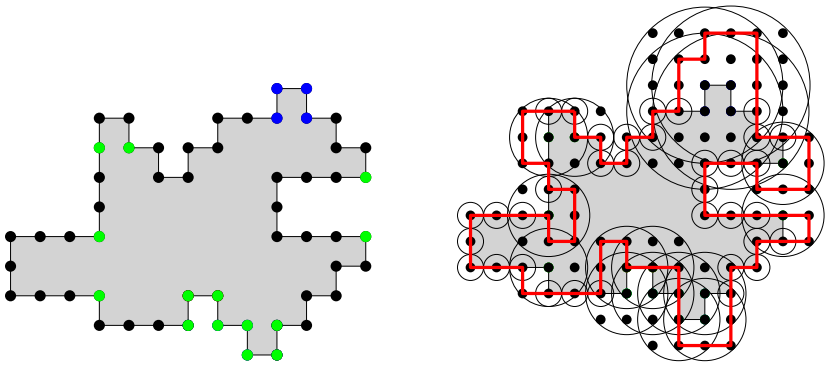

(a) (b)

Fig. 1. (a) Imprecise digital contour, color indicates the imprecision value assigned to each point: point p_i is black when $r_i = 1$, green when $r_i = 2$ and blue when $r_i = 3$. (b) Corresponding balls, with all digital points through which the ground truth $\mathcal{C}_0$ contour may pass.

2.1 Family of Tours

We denote by $B_i(p_i, r_i)$ the set of digital points included in the open Euclidean ball centered in p_i and of radius r_i. For the sake of simplicity, all indices on the points p_i are considered modulo n. Note that, since by hypothesis, for all i p_i and p_{i+1} are 4-connected, and all r_i are integers, if $r_i > r_{i+1}$ (or conversely), then $B_{i+1} \subset B_i$ (or conversely). If $r_i = r_{i+1} = r$, then if $r = 1$, $B_i \cap B_{i+1} = \emptyset$, otherwise $B_i \cap B_{i+1} \neq \emptyset$ and B_i and B_{i+1} are not included in one another.

Let $\cup B = \cup_i B_i$. Given the knowledge of the curve $\mathcal{C}$ and B, the first task is to define the family of curves which could be the curve $\mathcal{C}_0$. We call these curves *tours*.

A tour γ of $\mathcal{C}$ is a closed simple curve included in $\cup B$ that passes through the balls B_i in the "right order", so that the original order on the points p_i is somehow preserved in the tour. The precise definition is given below.

Definition 1 (gate). *The gate $G_{i,i+1}$ between the ball B_i and the ball B_{i+1} is the set of points in $B_i \cap B_{i+1}$ or the set of edges that connect a point of B_i to a point of B_{i+1} if B_i and B_{i+1} are disjoint.*

Definition 2 (tour). *A digital curve γ is a tour of $\mathcal{C}$ if and only if:*

- *it is a closed simple 4-connected curve included in $\cup B$;*
- *it can be decomposed into connected parts B_0 $G_{0,1}$ B_1 $\ldots$ $G_{i-1,i}$ B_i $G_{i,i+1}$ B_{i+1} $\ldots$ B_n $G_{n,0}$ B_0.*

This notion of tour is similar, but more restrictive, than the one introduced in [12] in the context of computational geometry. The curve depicted in red on Figure 1(b) is an example of a tour.

2.2 Definition of an Imprecise Shape: Points Labeling

Since tours are closed simple curves, Jordan theorem applies and the complementary of each tour is composed of two connected components : the closed one is the shape associated to the tour, the other one will be called its complementary. Any point in $\mathcal{S}$ is in one of the following classes:

- *inside points*: points that are in the shape associated with a tour for any tour ;
- *outside points*: points that are in the complementary of the shape associated with a tour for any tour ;
- *uncertain points*: points for which there exist two tours such that the point is in the shape for one of the tours, and in its complementary for the other one.

From the definition, tours are oriented: they must go from ball to ball following the order of the points of $\mathcal{C}$. In the following, we assume w.l.o.g. that the digital curve $\mathcal{C}$ is counter-clockwise oriented.

Definition 3 (valid arc). *A directed arc between two 4-connected digital points is valid if there exist a tour that uses this arc.*

Definition 4 (mandatory arc). *A directed arc xy is said to be mandatory if x belongs to a ball B_i of radius 1, y belongs to a ball B_{i+1} of radius 1.*

Proposition 1 (Necessary conditions). *A directed arc xy between two 4-connected points x and y is valid only if :*

(i) *xy is a mandatory arc. Note that the reverse arc yx is not valid ;*
(ii) *or x and y do not belong to any ball of radius one, and there exists an i such that either x and y belong to B_i or x belongs to B_i and y belongs to B_{i+1}.*
(iii) *or x belongs to a ball B_i of radius 1, y does not belong to any ball of radius 1 but belongs to the ball B_{i+1};*
(iv) *or y belongs to a ball B_i of radius 1, x does not belong to any ball of radius 1 but belongs to the ball B_{i-1}.*

The arcs verifying one of these properties are called graph arcs*.*

Proof. From Definition 2, if two successive balls B_i and B_{i+1} are both of radius 1, then the gate between these balls is reduced to the arc between the points p_i and p_{i+1}, and thus any tour must go through this arc, which is valid, and proves case (i).

Consider now an arc a between two 4-connected points x and y in $\cup B$, such that a does not fulfill any of the conditions above. We prove that this arc is not valid.

(i) Suppose that x and y do not belong to a ball of radius 1, and do not fulfill the other conditions of (ii). Then since they do not belong to a common ball, this arc cannot belong neither to a part B_i nor $G_{i,i+1}$ of the decomposition of a tour. Moreover, since there is no ball B_i such that x belongs to B_i and y to B_{i+1}, a can not link a point of B_i to neither a point from $G_{i,i+1}$ nor one from $G_{i-1,i}$ for all i. Then a cannot belong to any tour from Definition 2 and a is not valid.

(ii) Suppose that x belongs to the ball B_i of radius 1. Then, since there is no other point in B_i, any tour must go through x, and for any tour, the arc with source x must have a target y in B_{i+1}, otherwise the arc is not valid.

(iii) this case is similar to case (ii).

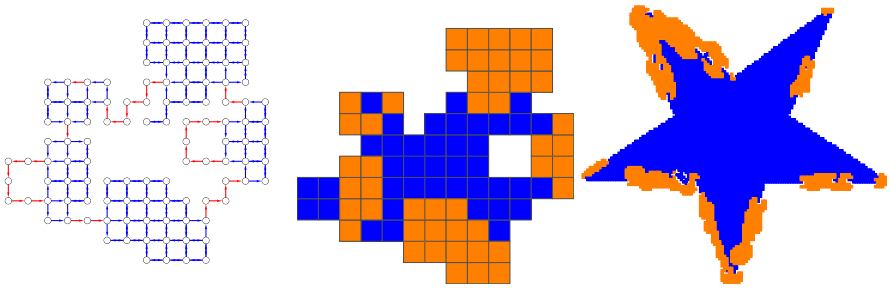

(a) (b) (c)

Fig. 2. (a) Graph arcs in blue, mandatory arcs in red for the imprecise digital contour depicted in Figure 1. (b)-(c) Inside points in blue, uncertain points in orange, outside points in white. In (c), the input imprecise digital contour is from $[10, 9]$: imprecision values are equal to the meaningful scale.

Note that the reciprocal is not true: some graph arcs may not be valid arcs, which means that for some of them, there may not exist a valid tour taking this arc. However, we have the following property :

Property 1. Mandatory arcs are valid arcs.

Figure 2(a) is an illustration of graph arcs and mandatory arcs for an imprecise digital contour. We now introduce some properties that enable to classify the pixels using these graph arcs.

Proposition 2 (diffusion). *Let p' be a pixel 4-connected to an inside pixel p, such that the linel shared by p and p' does not support a graph arc. Then p' is inside. (similar property if q' is 4-connected to q which is outside).*

Proof. Suppose p' is not inside. Then there exist a valid tour γ such that p' is outside. Since p is inside, p is in the shape associated to γ. Then, since γ is a valid tour, it is a simple closed curve, and thus a Jordan curve: any path between

inside and outside must cross γ. As a result, γ must go through the linel shared by p' and p, which is not possible since this linel does not support a graph arc.

This property shows that inside and outside points can be iteratively labelled from an initial point. In order to initialize the process, either some inside and outside points are known as part of the input, or we can use the following proposition.

Proposition 3 (initialization). *Let a be a mandatory arc, let p be the pixel to the left of a, and q the pixel to the right of a. Then p is inside and q is outside.*

Property 2. If the input curve $\mathcal{C}$ is a simple closed 4-connected curve, there is no pixel p which is both to the left and to the right of mandatory arcs.

These two propositions directly lead to an algorithm to label the pixels. If some pixels remain unlabelled after applying the initialization step and then the diffusion one, they are labelled as uncertain. Results of this labelling are presented in Figure 2(b)(c). We denote by $\mathcal{I}$ the set of inside points and $\mathcal{U}$ the set of uncertain points, and call **imprecise digital shape** the pair of sets $(\mathcal{I},\mathcal{U})$.

3 Volumetric Analysis

Any shape defined by a tour lies somewhere "in between" the digital shape defined by $\mathcal{I}$ and the digital shape defined by $\mathcal{I} \cup \mathcal{U}$. In the following, we present some tools to study this family of shapes.

3.1 Preliminary Definitions

Toleranced balls were introduced in [3] in the context of computational geometry for molecular modelling. They are defined as follows.

Definition 5 (Toleranced ball). *A toleranced ball $b(c, r^-, r^+)$ is a pair of concentric balls defined by a point c and two radii r^- and r^+ such that $0 \leq r^- \leq r^+$. We denote b^- (resp. b^+) the open ball of center c and radius r^- (resp. r^+).*

In the original setting, the constraint on r^- and r^+ was $0 < r^- < r^+$. But as we will see in the next paragraph, we need to relax this constraint in our framework. Given a collection $\mathcal{B}$ of toleranced balls, let $B^- = \cup_{b\in\mathcal{B}} b^-$ and $B^+ = \cup_{b\in\mathcal{B}} b^+$. We define a **filtration** of the shape B^+ as a nested sequence of shapes $B^- = S^0 \subseteq S^1 \subseteq \cdots \subseteq S^m = B^+$.

The sequence of shapes defining the filtration is parameterized using a function $\lambda_{\mathcal{B}} : \mathbb{R}^2 \to \mathbb{R}$ (later on, the function will be restricted to $\mathbb{Z}^2$). For a given $\lambda^i \in \mathbb{R}$, let us define the **λ^i-shape** as the set of points p such that $\lambda_{\mathcal{B}}(p) < \lambda^i$. For a given increasing sequence of values $0 = \lambda^0 < \lambda^1 < \cdots < \lambda^m$, the λ^i-shapes define a filtration of B^+ if and only if (i) λ^0-shape $= B^-$, (ii) for all i, λ^i-shape $\subseteq \lambda^{i+1}$-shape, and (iii) λ^m-shape $= B^+$.

The function $\lambda_{\mathcal{B}}$ can be seen as a function that governs the way toleranced balls grow from b^- to b^+. In the next section we show how to define (i) a collection $\mathcal{B}$ of toleranced balls from an imprecise digital shape and (ii) the function $\lambda_{\mathcal{B}}$.

3.2 Toleranced Balls of an Imprecise Digital Shape

Distance transformation is a classical tool in digital geometry and more generally image analysis for volumetric analysis. The distance transformation of a digital shape $\mathcal{S}$ consists in computing for each point of $\mathcal{S}$ the distance to the closest point in $\bar{\mathcal{S}}$. We denote $dt_{\mathcal{S}}(p) = \min_{q \in \bar{\mathcal{S}}}(d(p,q))$, where d is a distance on $\mathbb{Z}^2$. In [5], a very efficient algorithm is presented to compute the exact distance transformation for the Euclidean distance.

In our setting, the digital shape is imprecise, so that the distance between a point of the shape and its complementary is also imprecise. In this context, we define two distance transformations : $dt_{\mathcal{I}}$ and $dt_{\mathcal{I}\cup\mathcal{U}}$. For each point p in $\mathcal{I}$ these distance transformations provide information on the lowest and the greatest possible distance between p and a point in $\bar{\mathcal{S}}$ for any shape $\mathcal{S}$ associated to a tour. For any point p in $\mathcal{U}$, the distance transformation $dt_{\mathcal{I}\cup\mathcal{U}}(p)$ is the shortest distance between p and a point of $\bar{\mathcal{S}}$ for any shape $\mathcal{S}$ associated to a tour and that contains p.

We use these two distance transformations to define a toleranced ball for each point $p \in \mathcal{I} \cup \mathcal{U}$ as follows. For any point p in $\mathcal{I}$ we define the toleranced ball $b(p, dt_{\mathcal{I}}(p), dt_{\mathcal{I}\cup\mathcal{U}}(p))$. Similarly, for any point p in $\mathcal{U}$ we define the toleranced ball $b(p, 0, dt_{\mathcal{I}\cup\mathcal{U}}(p))$. Taking a look back at Definition 4, we note that in this case, we may have $r^- = dt_{\mathcal{I}}(p) = dt_{\mathcal{I}\cup\mathcal{U}}(p) = r^+$, and for toleranced balls centered on uncertain points, we have $r^- = 0$.

The collection of all the toleranced balls thus defined for a given imprecise digital shape is denoted by $\mathcal{B}$. By construction, for any $b \in \mathcal{B}$, the open ball $b^-(c, r^-) \subset I$ and the open ball $b^+(c, r^+) \subset \mathcal{I}\cup\mathcal{U}$. With the notations introduced in the previous section, we have $B^- = \mathcal{I}$ and $B^+ = \mathcal{I} \cup \mathcal{U}$ (see Figure 3(a)).

3.3 Distances

In order to define the function $\lambda_{\mathcal{B}}$ which governs the ball growing process, the first thing is to specify the distance between a toleranced ball and a point. Several distances can be defined. In [3], they use the additively-multiplicatively distance which make each ball grow linearly with respect to the difference between r^- and r^+. This definition assumes that $r^- \neq r^+$.

Definition 6 (additively-multiplicatively distance). *Let $b(c, r^-, r^+)$ a toleranced ball, p a point, and d the Euclidean distance between points of $\mathbb{Z}^2$. Then $d_{am}(b, p) = \frac{d(p,c) - r^-}{r^+ - r^-}$.*

This distance is actually based on the additively weighted distance between a ball $b(c, r)$ and a point p defined as $d(c, p) - r$. The additively-multplicatively distance is associated with the so-called compoundly-weighted Voronoi diagram [13], which falls in the class of non-linear Voronoi diagrams (bissectors are not linear).

In our framework, some of the toleranced balls may have equal radii, so that we have to take this case into account in the distance definition. When the two

radii of the toleranced ball are equal, the ball does not grow (nor deflate), and then can never touch a given point p which is not on its boundary.

Let d_b be a distance between a ball b and a point p, such that $d_b(b,p) < 0$ if $p \in b$, $d_b(b,p) = 0$ si $p \in \partial b$ and $d_b(b,p) > 0$ if $p \notin b$. We propose a new distance between a toleranced ball and a point, that generalizes the additively-multiplicatively distance and introduces a threshold.

Definition 7. *Let $b(c, r^-, r^+)$ a toleranced ball, p a point and d_b a distance between a ball and a point. Then the function $d_{tb} : \mathcal{B} \times \mathbb{Z}^2 \to \mathbb{R}$ is defined as :*

$$d_{tb}(b,p) = \begin{cases} +\infty & \text{if } p \notin b^+ \\ -\infty & \text{if } p \in b^- \\ \frac{d_b(b^-,p)}{d_b(b^-,p) - d_b(b^+,p)} & \text{if } b^- \neq b^+ \\ 0 & \text{if } b^- = b^+ \text{ and } d_b(b^-,p) = 0 \end{cases}$$

We recall that the power distance between a ball $b(c,r)$ and a point p is given by $d(c,p)^2 - r^2$. Injecting this distance in the generalized distance defined above, we can make the balls grow linearly with respect to the difference between the squares of the two radii.

However, we have to keep in mind that we have actually two types of toleranced balls : some toleranced balls which center is in $\mathcal{I}$ and others for which the center lies in $\mathcal{U}$. If we make all these balls grow simulaneously using the d_{tb} distance, the balls centered on uncertain points will start to grow at the same time as the balls centered on inside points. So that if the distance d_{tb} is used straightforwardly to define $\lambda_{\mathcal{B}}$, shapes may grow in an unexpected way. In order to take into consideration these different types of balls, we introduce an index η which controls the moment a given toleranced ball begins to grow (see Figure 3(b)).

Definition 8 (Index). *Given a imprecise digital shape $(\mathcal{I},\mathcal{U})$ and its collection of toleranced balls $\mathcal{B}$, we define the index $\eta : \mathcal{I} \cup \mathcal{U} \to \mathbb{Z}^+$ as :*

$$\eta(p) = \begin{cases} 0 & \text{if } \exists b \in \mathcal{B},\ p \in b^-, \\ 1 & \text{if } \exists b \in \mathcal{B},\ b^- \neq \emptyset \text{ and } p \in b^+ \setminus b^- \\ \min_{b(c,r^-,r^+) \in \mathcal{B}} \{\eta(c) + 1 \mid p \in b^+\} & \text{otherwise.} \end{cases}$$

For some specific points in $\mathcal{U}$, the recursive definition above may not converge. Indeed, consider for instance a point $p \in \mathcal{U}$ such that its toleranced ball is $b(p,0,1)$ and p belongs to no other toleranced ball. In this case, the recursive step loops. To overcome this particular case, we define a maximal value $\hat{\eta}$ for η, which is equal to the maximum of the well defined values $\eta(p)$ plus one.

We put together the index and the distance d_{tb} to define a new distance λ.

Definition 9. *Let d_{tb} be the distance defined in Definition 6 and η the index map defined in Definition 7. Then the function $\lambda : \mathcal{B} \times \mathbb{Z}^2 \to \mathbb{R}$ is defined as :*

$$\lambda(b, p) = \eta(c) + d_{tb}(b, p)$$

.

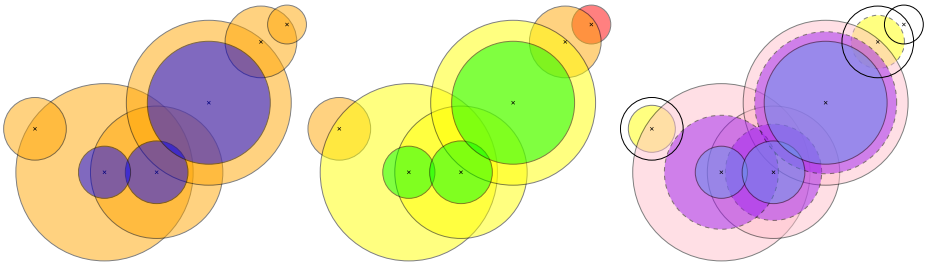

(a) (b) (c)

Fig. 3. (a) Set B^- in blue, B^+ in orange and blue ; (b) Indices : 0 for points in green, 1 for points in yellow, 2 for points in orange and 3 for points in red ; (c) λ-shapes using the additively weighted distance : for $\lambda = 0$ in blue, $\lambda = 0.5$ in purple and blue, $\lambda = 1$ in pink, purple and blue and $\lambda = 1.75$ in yellow, pink, purple and blue.

3.4 Toleranced Balls Growing Process

We can now introduce the growth-governing function $\lambda_{\mathcal{B}}$.

$$\begin{aligned} \lambda_{\mathcal{B}} \colon \mathbb{Z}^2 &\to \mathbb{R} \\ p &\mapsto \min_{b \in \mathcal{B}} \lambda(b, p). \end{aligned}$$

Proposition 4. *Given an imprecise shape $(\mathcal{I},\mathcal{U})$ and the collection $\mathcal{B}$ of its toleranced balls, the λ^i-shapes defined using function $\lambda_{\mathcal{B}}$, with an increasing sequence of λ^i, with $\lambda^0 = 0$ and $\lambda^m = \hat{\eta} + 1$ defines a filtration of $\mathcal{I} \cup \mathcal{U}$.*

Proof. First, we prove that the λ^0-shape is equal to $B^- = \mathcal{I}$. Let p be a point in $\mathcal{I}$, and consider the toleranced ball $b(p, r^-, r^+)$ centered on p. By definition, $b \in \mathcal{B}$, and we have $d_b(b^-, p) < 0$. Then, $\lambda_{\mathcal{B}}(p) < 0$ and p belongs to the λ^0-shape. Conversely, let p be a point such that $\lambda_{\mathcal{B}}(p) < 0$. This implies that there exist a toleranced ball $b(c, r^-, r^+) \in \mathcal{B}$ such that $d_{tb}(b, p) < 0$ and $\eta(c) = 0$. Thus, p belongs to a ball $b^-(c, r^-)$ with $c \in \mathcal{I}$, which proves that p belongs to $\mathcal{I}$.

Proving that for all i and $\lambda^i < \lambda^{i+1}$, the λ^i-shape is included in the λ^{i+1}-shape is straightforward since a λ^i-shape is defined as threshold on the $\lambda_{\mathcal{B}}$ function.

Last, we shall prove that the λ^m-shape with $\lambda^m = \hat{\eta}+1$ is equal to $B^+ = \mathcal{I} \cup \mathcal{U}$. Let $p \notin \mathcal{I} \cup \mathcal{U}$. Then for all $b \in \mathcal{B}$, $p \notin b^+$, so that $d_{tb}(b,p) = +\infty$ for all b, and thus $\lambda_{\mathcal{B}}(p) = +\infty$ and $p \notin \lambda^m$-shape. Conversely, let $p \in \mathcal{I} \cup \mathcal{U}$. Then there exist $b \in \mathcal{B}$ such that $p \in b^+$. If $p \in b^-$, then $\lambda_{\mathcal{B}}(p) = -\infty$ and $p \in \lambda^m$-shape. Otherwise, for any $b(c_0, r^-, r^+) \in \mathcal{B}$ such that $p \in \mathcal{B}$, we have $\eta(c_0) \leq \hat{\eta}$ and $d_{tb}(b,p) < 1$. As a result, $\lambda_{\mathcal{B}}(p) < \hat{\eta} + 1$ and $p \in \lambda^m$-shape.

Let us study a little bit more in details which balls compose λ^i-shapes. Given a toleranced ball $b(c, r^-, r^+)$, the ball b grown by a factor α is defined as $b_\alpha = \{p \mid d_{tb}(b,p) < \alpha\}$. If the distance between balls and points is the additively weighted distance, then $b_\alpha = b(c, r^- + \alpha(r^+ - r^-))$. If the power distance is used, then $b_\alpha = b(c, {r^-}^2 + \alpha({r^+}^2 - {r^-}^2))$. Then we have :

Proposition 5. *Given an imprecise shape $(\mathcal{I},\mathcal{U})$ and the collection $\mathcal{B}$ of its toleranced balls, the λ^i-shape is equal to*

$$\Big(\bigcup_{b\in\mathcal{B},\eta(c)<\lfloor\lambda^i\rfloor} b^+\Big) \cup \Big(\bigcup_{b\in\mathcal{B},\eta(c)=\lfloor\lambda^i\rfloor} b_{\lambda^i-\lfloor\lambda^i\rfloor}\Big)$$

Proof. Let p be a point in the λ^i-shape. This is equivalent to say that there exist a toleranced ball $b(c, r^-, r^+) \in \mathcal{B}$ such that $\eta(c) + d_{tb}(b,p) < \lambda^i$. Only two cases are possible :

1. either $\eta(c) < \lfloor\lambda^i\rfloor$ and $dt_{tb}(b,p) < 1$, so that $p \in b^+$:
2. or $\eta(c) = \lfloor\lambda^i\rfloor$ and $dt_{tb}(b,p) < \lambda^i - \lfloor\lambda^i\rfloor$ and thus $p \in b_{\lambda^i-\lfloor\lambda^i\rfloor}$.

An illustration of a sequence of λ-shapes for a given collection of toleranced balls is given in Figure 3 (c), for $\lambda^0 = 0$, $\lambda^1 = 0.5$, $\lambda^2 = 1$ and $\lambda^3 = 1.75$. Figure 4(c) shows the λ-shapes for the same sequence of λ^i for the imprecise digital Star shape. Moreover, in Figure 4(a) and (b) we can see the difference between two growth models using the additively weighted distance in (a) and the power distance in (b) (for λ values equal to $0.2, 0.5, 0.7$ and 0.9).

3.5 Compact Representation of the Filtration

The $\lambda_{\mathcal{B}}$ function defined in the previous section gives an information, for each point of the imprecise digital shape, on the instant this point will be reached during the ball growing process. The collection $\mathcal{B}$ of toleranced balls used in this process counts exactly one toleranced ball per point of the imprecise digital shape. However, during the growing process, some of these toleranced balls may never be the first to reach a point of the shape. As a result, these toleranced balls carry redundant information about the imprecise digital shape and could be discarded.

Definition 10 (λ-Voronoi Map). *Given a collection $\mathcal{B}$ of toleranced balls, the λ-Voronoi region of a ball $b \in \mathcal{B}$ is defined as $R_b = \{p \mid \lambda(b,p) < \lambda(b',p)\ \forall b' \in \mathcal{B}\}$.*

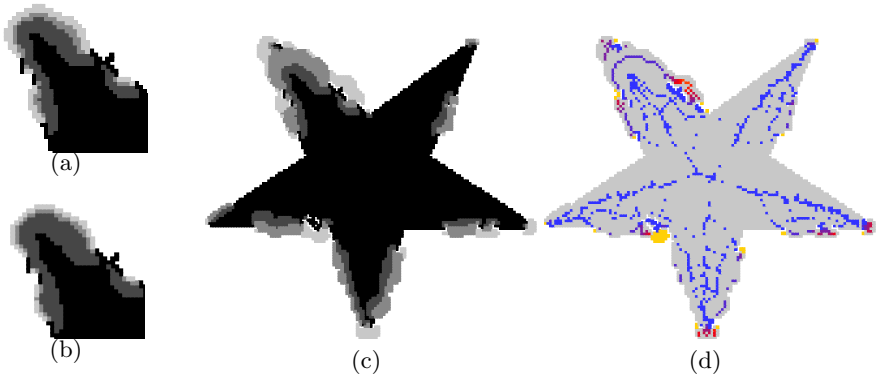

Fig. 4. (a)-(b) λ-shapes obtained for $\lambda \in \{0.2, 0.5, 0.7, 0.9\}$ using the additively weighted distance in (a) and the power distance in (b) ; (c) λ-shapes for $\lambda \in \{0, 0.5, 1, 1.75\}$ using the additively weighted distance ; (d) Sites extracted from the λ-Voronoi Map based on the additively weighted distance. The colormap from blue to red and then yellow represents the level τ of each site.

The λ-Voronoi Map is defined on the set of points B^+ for a given collection of toleranced balls $\mathcal{B}$. The set of regions is a tessellation of B^+.

Definition 11 (Sites). *Given a collection $\mathcal{B}$ of toleranced balls, a* site *is a toleranced ball with a non empty λ-Voronoi region. The level τ of a site b_s is defined as $\tau(b_s) = min\{\lambda(b_s, p) \mid p \in R_{b_S}\}$.*

This approach is similar to the extraction of the medial axis from the squared Euclidean distance transformation [5] : the points of the medial axis are the ones with a non empty region in the power diagram defined with all the balls computed from the distance transformation. Similarly to the medial axis, it is straightforward to show that any λ-shape can be reconstructed from the set of sites (see Figure 4(d) for an illustration).

Proposition 6 (Reconstruction). *Given a collection $\mathcal{B}$ of toleranced balls, any λ^i-shape can be reconstructed from the set of sites b_s such that $\tau(b_s) < \lambda^i$ using Proposition 5.*

4 Discussion

In this paper, we introduced a new framework to undertake contour and volumetric analysis of digital shapes taking into account the imprecision of the input data. To conclude, we would like to open the discussion on several key points and potential perspectives.

Model Section 3 was devoted to the definition of a growth model based on the d_{tb} distance function. Using this function, the growth speed of each toleranced ball depends somehow on the difference between the two radii. We could easily define a similar function that would lead to a uniform growth speed for all the balls. With such a setting, we may build on well-known results on the Voronoi Diagram stability through growth process. Indeed, if the rule to grow each ball is to increase the square radius r^2 to $r^2 + t$ at time t, then the Power Voronoi Diagram of these balls is constant at all times [7].

Finally, every growth model leads to different λ^i-shapes and there is a need to define criteria (maybe depending on the application) to compare these models.

Algorithms The results were obtained using brute-force algorithms, which leads to a worst-case complexity of $\mathcal{O}(n^2)$ for an image with n pixels for all the computations (graph, λ values, sites). When volumetric analysis is concerned, all comes down to the computation of the λ-Voronoi Diagram for a collection of toleranced balls. Indeed, the λ values for each point can be easily retrieved from this diagram. Unfortunately, the distance λ used to compute the λ-Voronoi diagram is not separable [4] so that very efficient separable algorithms cannot be applied straightforwardly.

Implementation Algorithms were implemented using the open-source libraries DGtal [1] for the digital geometry part, and Lemon [2] for the graph part. In particular, distance transformations were computed using the state-of-the-art algorithm from [5] available in DGtal. However, the distance introduced in this work involve non integer computations, that may lead to incorrect results (for instance incorrect reconstruction) due to unintentional rounding operations.

To go further The second part of this work about volumetric analysis could actually be applied to other imprecise digital shapes inputs : the only requirement is for the imprecise digital shape to be defined by a set of inside points, and a set of uncertain points. One could imagine to extract this kind of information using a segmentation algorithm on gray level images. Similarly, this volumetric study may also be extended to 3D imprecise digital shapes quite easily.

Finally, an ultimate objective when volumetric analysis is concerned is to compute the medial axis of the shape. A first step towards the definition of the medial axis of an imprecise digital shape could be to compute the medial axis for well chosen sample of λ^i-shapes, and study the evolution of the positions and radius of the centers computed.

References

1. DGtal: Digital Geometry Tools and Algorithms Library. `http://dgtal.org`
2. Lemon Graph Library. `https://lemon.cs.elte.hu/trac/lemon`
3. Cazals, F., Dreyfus, T.: Multi-scale geometric modeling of ambiguous shapes with : Toleranced balls and compoundly weighted alpha-shapes. Comput. Graph. Forum 29(5), 1713–1722 (2010)

4. Coeurjolly, D.: 2d subquadratic separable distance transformation for path-based norms. In: Discrete Geometry for Computer Imagery, DGCI. Lecture Notes in Computer Science, vol. 8668, pp. 75–87. Springer (2014)
5. Coeurjolly, D., Montanvert, A.: Optimal separable algorithms to compute the reverse euclidean distance transformation and discrete medial axis in arbitrary dimension. IEEE Trans. Pattern Anal. Mach. Intell. 29(3), 437–448 (2007)
6. Debled-Rennesson, I., Feschet, F., Rouyer-Degli, J.: Optimal blurred segments decomposition of noisy shapes in linear time. Computers & Graphics 30(1), 30–36 (2006)
7. Goodman, J.E., O'Rourke, J. (eds.): Handbook of Discrete and Computational Geometry. CRC Press, Inc. (1997)
8. Jooyandeh, M., Mohades, A., Mirzakhah, M.: Uncertain voronoi diagram. Information Processing Letters 109(13), 709 – 712 (2009)
9. Kerautret, B., Lachaud, J.: Meaningful scales detection along digital contours for unsupervised local noise estimation. IEEE Trans. Pattern Anal. Mach. Intell. 34(12), 2379–2392 (2012)
10. Kerautret, B., Lachaud, J.: Meaningful scales detection: an unsupervised noise detection algorithm for digital contours. IPOL Journal 4, 98–115 (2014)
11. Lindblad, J., Sladoje, N.: Linear time distances between fuzzy sets with applications to pattern matching and classification. IEEE Transactions on Image Processing 23(1), 126–136 (2014)
12. Löffler, M.: Data Imprecision in Computational Geometry. Ph.D. thesis, Utrecht University (2009)
13. Okabe, A., Boots, B., Sugihara, K.: Spatial Tessellations: Concepts and Applications of Voronoi Diagrams. John Wiley & Sons, Inc. (2000)
14. Sladoje, N., Nyström, I., Saha, P.K.: Measurements of digitized objects with fuzzy borders in 2d and 3d. Image Vision Comput. 23(2), 123–132 (2005)
15. Veelaert, P.: Graph-theoretical properties of parallelism in the digital plane. Discrete Applied Mathematics 125(1), 135–160 (2003)